ISSN 0029-3865

CBPF-NF-031/84

STRUCTURE VARIATIONS OF CARBONIZING LIGNIN

by

C. OTANI*, H.A. POLIDORO*, S. OTANI* and
A. CRAIEVICH[1]

[1] Centro Brasileiro de Pesquisas Físicas - CNPq/CBPF
Rua Dr. Xavier Sigaud, 150
22290 - Rio de Janeiro, RJ - Brasil

Instituto de Física e Química de S. Carlos
13560 - São Carlos, São Paulo - Brasil

* Centro Técnico Aeroespacial - IPD-PMR
12200- São José dos Campos, São Paulo - Brasil

STRUCTURE VARIATIONS OF CARBONIZING LIGNIN

C. OTANI*, H.A. POLIDORO*, S. OTANI* and A. CRAIEVICH**

*Centro Técnico Aeroespacial - IPD-PMR
São José dos Campos, S. Paulo - Brazil

**Centro Brasileiro de Pesquisas Físicas
Rio de Janeiro, RJ - Brazil and

Instituto de Física e Química de S. Carlos
São Carlos, São Paulo - Brazil

ABSTRACT

The studied lignin is a by-product of the process of ethanol production from eucaliptus. It was heat-treated under inert atmosphere conditions at increasing temperatures from 300 C up to 2400C. The structural variations were studied by wide-angle X-ray diffraction, small-angle X-ray scattering and infrared absorption spectroscopy. The bulk and "real" density of the compacted materials have also been determined as functions of the final temperature. These experimental results enabled us to establish a mechanism of structure variation based on the formation of a turbostratic graphite-like and porous structure within the initially amorphous lignin matrix.

Key-words: Lignin; Coke; Carbonisation.

1 INTRODUCTION

Lignin is a polymeric tridimensional molecule forming an important part of natural wood (between 25 and 30% by weight). Its molecular structure is not completely known because of the chemical reactions occuring during the separation process. The accepted molecular model is based on short linear chains cross-linked in a variety of ways to build an "infinite" three dimensional structure[1].

Pyrolysis of isolated lignin leads to a porous carbonaceous material (lignin coke) which is in many aspects similar to the final product of the pyrolysis of wood (charcoal).

We are interested in structural variations of lignin when heated at increasing temperatures in an inert atmosphere. The lignin studied in this work is a by-product of ethanol production from eucalyptus wood. The variations in density and electrical conductivity of this material were also studied with a view on eventual technological applications[2].

The variations in density (bulk and "real"), local molecular structure, macroscopic porosity, submicroscopic porosity and electrical resistivity have been studied as functions of the maximum temperature of heat-treatment. Features related to the molecular structure have been determined by wide angle x-ray diffraction and infra-red absorption spectroscopy. The coarse and submicroscopic porosity have been investigated by ordinary microscope and small angle x-ray scattering, respectively. Finally we tried to correlate the variations in macroscopic properties to the structure changes during lignin pyrolysis.

2 EXPERIMENTAL

2.1 Sample preparation

Lignin samples were first powdered to -200 mesh and then granulated by diluting in water and passing the solution through different mesh size sieves. The final granulometric composition was the following: 64, 2% of -60 and +80 mesh, 5% of -150 and +200 mesh and 30,8% of -200 mesh. Disc shaped samples were prepared by hydraulic pressure over a cylyndric dye filled with the pellets.

The samples were heated up to 1000C using a tubular standard electrical furnace, in an argon atmosphere. From 1000 up to 2400C, a furnace with graphite resistance was used. All heat treatments were done with the samples immersed in 99% pure natural graphite powder. The heating rates were 1000C/24 hrs and 600 C/h for treatments at temperatures lower and higher than 1000C, respectively. The choice of these heating rates was based on a preliminary study of the influence of heating rate on physical properties of carbonaceous materials obtained from lignin[2].

2.2 Density and coarse porosity measurements

The mass loss of all the samples was determined before and after heat treatment by weighting dried samples (kept at 105 C during 2 h. in air, and cooled in a sealed dissecator). The variation in bulk density was determined from the variations in weight and total volume of the samples.

In order to determine the "real density" of the heat treated material the "sink and float" method[3] was employed on powdered samples. The solvents used for determination of density in the range from 1.20 to 1.60 g/cm^3 were mixtures of toluene and carbon tetrachloride. For samples with densities ranging from 1.60 to 2.00 g/cm^3 mixtures of 1,2 - dibromoethane and carbon tetrachloride were used.

The coarse porosity of the samples was determined indirectly through the measured values of "real" and bulk densities, using the following equation:

$$\text{Porosity } (\%) = \left(1 - \frac{D_A}{D_R}\right) 100\%, \qquad (1)$$

where D_R and D_A are the real and bulk density, respectively.

2.3 Techniques

Spectrophotometric measurements of materials heat-treated up to 1000C, were carried out with samples of 0.1 weight percent of lignin in a KBr matrix, using a Perkin Elmer 283B infrared Spectrometer. The samples were mounted in a polyester resin matrix and polished. An Olympus BHT optical microscope with a polarization attachment was used for the analysis of the coarse porosity.

The wide angle x-ray diffraction patterns of every sample were obtained using a standard Phillips X-ray powder diffractometer with KαCu radiation, monochromatized by a graphite monochromator. The heat treated lignin disks did not receive

any further preparation for the x-ray diffraction measurements.

The small angle x-ray scattering (SAXS) study were done at the synchrotron radiation laboratory L.U.R.E. (Orsay). The white synchrotron radiation was monochromatized by a bent germanium crystal to obtain a monochromatic beam with wavelength λ=1.608Å. The high intensity of the beam enabled us to use pin-hole collimation, avoiding desmearing corrections of SAXS data. A linear position sensitive detector was used to record the SAXS intensity. At very small angles the scattered intensity by lignin is very high and decreases rapidly with the scattering angle. The synchrotron source was useful to obtain accurate data in the outer part of the scattering curve of weak intensity. Appropriate copper foils were used to attenuate the scattered radiation in the lower angular domain to avoid detector saturation. From the total SAXS curve the parasitic scattering was subtracted. The resulting curves were normalized to equivalent sample absorption and thickness and incident beam intensity.

The electrical resistivity measurements were carried out by the four point method. The samples were not specially prepared for these measurements. The electrical resistance between two points equidistant from the center of the disk shaped samples, was measured at room temperature. The resistance obtained in ohms was multiplied by the maximum cross section area and divided by the distance separating the two measuring electrodes. This value was corrected to account for the difference between the real effective cross-section area and the measured one. Hence the resistivity was determined by means of the following empirical equation:

$$\rho(\Omega cm) = \frac{V_m}{I} \frac{D\,E}{L} (0,779) \qquad (2)$$

where V_m is the measured voltage, I the electrical current, D the sample diameter, E the sample thickness and L the distance between electrodes. The resistivity of samples heat-treated below 1000C is much higher than the maximum value detectable by the four point method. Therefore we measured it with a megaohmeter by the two-point method.

3 RESULTS AND DISCUSSION

The mass loss, volume shrinkage, fraction of coarse porosity and bulk density variations are plotted as functions of heat treatment temperature in Figure 1. These curves show two temperatures ranges (near 500 and 1700 C) at which the volatilization process is not compensated by volume shrinkage. This observation was quantitatively confirmed by examining micrographies of samples treated at increasing temperatures. The obtained micrographies show that samples treated up to about 500 C and 1700C present a fraction of porosity volume larger than those of other samples.

The transformations during carbonization up to 1000C were studied by infra-red absorption spectroscopy. The spectra obtained at room temperature from as received lignins and those heat treated at 300, 500, 700 and 1000C are presented in Figure 2. The infra-red spectrum obtained from samples without heat treatment shows many peaks which can be assigned to in-

fra-red absorption of lignin molecules as reported by Hergert[4]. All these peaks decrease in intensity as the heat treatment temperature increases, showing that organic chemical bonds are broken and molecular groups are volatilized. The last curve in Figure 2, which is completely flat, represents the spectrum of the sample treated at 1000C. The absence of any spectroscopic structure means that at 1000C the fraction of molecular groups present in the samples is too low to be detected by this technique. This allows us to conclude that a 1000C lignin is almost entirely carbonized.

The x-ray diffraction pattern of lignin without heat treatment (curve RT in Figure 3) shows the broad peak which is characteristic of amorphous materials. The Bragg angle θ_m associated with the maximum of the main peak is related to an average distance a between neighboring atoms by means of the Ehrenfest equation[5]:

$$1.23\,\lambda = 2d\,\mathrm{sen}\theta_m \qquad (3)$$

The distance d is equal to 5.20Å for T = 300C and decreases for increasing temperatures. The shift of peak maxima indicates that some progressive molecular ordering occurs, diminishing the average first-neighbor distance at increasing heat treatment temperature. X-ray diffraction patterns from samples heat treated at 1000C show the presence of a new peak at an angular position which corresponds approximately to the (10) reflection of a turbostratic graphitic structure. This shows that at 1000C small hexagonal layer units are already formed. These layers do not

show interlamellar ordering since no sharp (002) reflection of graphitic structure is apparent at this temperature. The two sharp additional peaks at 32 and 45 degrees do not correspond to graphitic reflections. These peaks were associated with the formation of crystalline aggregates of impurity elements. In order to investigate the influence of impurity elements on the physical properties of the final products, we are performing new structure studies on purified lignins.

When the heat treatment temperature is raised up to temperatures above 1000C, a slowly increasing peak near to the (002) lamellar peak can be observed. This peak overlaps the original broad band, indicating that a fraction of the amorphous matrix is transforming into a stack of graphitic layers.

The formation of a layered structure can also be verified by the fact that the (10) peak, already present in the diffraction pattern of the sample treated at 1000 C becomes more pronounced at increasing temperature, and at 2400 C it becomes clearly assymetric. We attribute these variations to the progressive formation of a turbostratic structure (a disordered packing of hexagonal lammellaes). The additional peak in the diffraction pattern of samples treated at 2400C corresponds to the (004) reflection of the layered system. Finally, it can also be pointed out that diffraction peaks from impurity aggregates become very weak above 2000C, implying that the impurity elements are volatilized or dissolved below this temperature. This confirms the existence of a second stage of volatilization of elements heavier than those volatilized below 1000C.

No attempt of quantitative determination of the fraction

of amorphous material has been done, since the variations in the diffraction patterns do not indicate a simple two-phases structure. The transformation seems to be discontinuous in the early stages (1400C) at which the (002) peak appears, but at higher temperatures there is a mixture of small graphitic crystals (producing a rather large 002 peak) and an amorphous matrix showing incresing degree of ordering (increase in the angular position of the maximum of the broad band).

The set of SAXS curves are shown in log-log scale in Figure 4. We can observe in this figure the important variation of SAXS intensity from low to high angles (four order of magnitude). The SAXS curves present features which are similar to those observed in natural wood[7], glassy carbon[8] and carbon fibers[9,10]. The curves corresponding to low temperatures, present an essentially linear behavior indicating a potential dependence between the intensity and the scattering angle. SAXS curves corresponding to higher heat treatment temperatures also present a potential variation at small angles, a shoulder at medium angles and again a potential dependence at higher angles.

A potential dependence of SAXS intensity is expected from a two-electronic density system with sharp interfaces. If the system is composed by a porous structure in a nearly homogeneous matrix, the SAXS intensity I(h) can be approximated at high angle by Porod's law[11]:

$$I(h) = 2\pi\rho^2 \frac{S}{h^4} \qquad (4)$$

where ρ is the mean electronic density of the matrix, S the surface area of the interface matrix-pores and h the modulus of the scattering vector ($h \simeq 4\pi \frac{\theta}{\lambda}$, θ being half of the scattering angle and λ the X-ray wavelength).

We can see in the log-log plot of Figure 4 that SAXS from samples treated at 300 and 400C obey Porod's law, since the slope of the linear region is close to -4. A positive deviation from Porod's law is observed in the outer part of the SAXS curve. The SAXS intensity from these samples has been attributed to the contribution from the coarse porosity existing in the precursor lignin.

The shoulder in the SAXS curves which develops at increasing temperatures is similar to the observed in charcoal[6]. As it was pointed out by Schmidt[12] the presence of a shoulder in a log-log plot can be attributed to the progressive generation of micropores in the matrix at increasing temperatures. The qualitative analysis of the SAXS curves indicates that the increase in heat treatment temperature produces an increase in the SAXS intensity and a decrease in the angular position of the shoulder.

The analysis of the features of microporosity has been done using Guinier's law[11]. It holds for dispersed systems of "particles" (or pores) in a homogeneous matrix. In the case of micropores it can be written as:

$$I(h) = N\rho^2V^2 e^{-\frac{1}{3} R^2h^2} \qquad (5)$$

where N is the number of micropores, ρ the electronic density of the matrix, V an average volume of the pores and R their average radius of gyration.

Assuming that the contribution from the coarse porosity to SAXS intensity within the angular domain of validity of Guinier's law can be neglected, we plotted the data in log I vs h^2 scale (Figure 5) to determine, from the slope of the linear region, the average radius of gyration of the pores.

The extrapolation of the linear part of Guinier's plot towards zero angle, provides a way to determine the variation of the number of pores in the sample. Assuming a simple model of spherical pores equations 5 yields:

$$N \alpha I(0)/R^6 \qquad (6)$$

The values of the average radius of gyration R and the variation of number of pores N are represented in Figure 6. We conclude from SAXS results that micropores begin to be detected above 700C. Their size increases at slower rate up to 1700 C and faster above this temperature. The number of pores is approximately constant from 700 C up to 1700 C and decreases sharply above this temperature. The increase in size of micropores was also observed in carbonized natural woods by Schmidt et al.[6].

The "real" density of the samples is represented as a function of temperature in Figure 7. The method of measurement of "real" density eliminates the effect of the coarse porosity and gives information related to structural variations in the carbonaceous matrix and to the associated microporosity. A rapid increase in real density is observed up to 1000C. followed by a almost constant value up to about 1800C and a second increase

above this temperature.

The electrical resistivity at room temperature of lignin samples is also presented in Figure 7 as a function of the heat treatment temperature. We can note a very rapid decrease in resistivity up to 1000C, an approximately constant value between 1000 and 2000C and a second decrease at higher temperatures.

4 CONCLUSIONS

The present experimental results using the various experimental techniques, suggest that structural variations in lignin heated at increasing final temperatures are characterized by three definite stages.

During the first stage from room temperature to about 1000C, volatilization of the light elements occurs and a coarse porous structure develops. Near the end of this stage, the polymeric chains form small graphitic lamellae inducing a rapid variation of electric conductivity from values characteristic of insulators to those of semiconducting materials. The formation of the small graphitic lamellae is accompanied by a densification of the matrix and a simultaneous formation of micropores in the incipient graphitic phase.

During the second stage, the heavier elements volatilise, the size of micropores increases at a moderate rate, but the number remains constant, and the matrix progressively evolves from a predominantely amorphous structure to a turbostratic

graphite - like structure. These changes do not produce appreciable variation in real density and electrical resistivity of the material. We can understand this by assuming that, in regions where the turbostratic structure develops, the local densification of the matrix is compensated by the growth of existing pores with no appreciable resultant variation in the average "real" density. The constancy of electrical resistivity would be due to the isolated nature of these higher conductivity regions.

The third stage is characterized by the presence of a predominant fraction of the matrix having a turbostratic graphite-like structure and a decreasing number of growing micropores. This opposite variation of R and N suggests the activation of a mechanism of coalescence of pores. These structural variations produce an expected decrease in electrical resistivity, since the high conductivity isolated regions become progressively interconnected. The increase in real density is a consequence of the closer stacking of graphitic lamellaes.

Additional studies on the influence of sample purity and heating rate on the structure and physical properties of lignin are in progress.

5 ACKNOWLEDGEMENTS

We are grateful to Yvonne Mascarenhas for helpful discussions, to FTI-INT for providing the lignin samples and FIPEC and SUBIN for their support. We also thank the synchrotron radiation laboratory LURE the beam time for SAXS experiments.

FIGURE CAPTION

Fig. 1 - Variations in coarse porosity (a), bulk density (b), volume (c), and mass (d) as a function of heat treatment temperature.

Fig. 2 - Infra-red absorption spectra of lignin samples heat treated at the indicated temperatures (Celsius scale), and at the room temperature (RT).

Fig. 3 - Wide angle x-ray diffraction patterns corresponding to samples heat treated at the indicated temperatures (Celsius scale).

Fig. 4 - Small angle x-ray scattering curves from lignin samples heat treated at the indicated temperatures (Celsius scale) plotted in log - log scale.

Fig. 5 - Guinier plots of the small angle x-ray scattering results. Heat treatment temperatures are in Celsius scale.

Fig. 6 - Average radius of gyration and number of micropores as functions of the heat treatment temperature.

Fig. 7 - Electrical resistivity and real density as functions of heat treatment temperature.

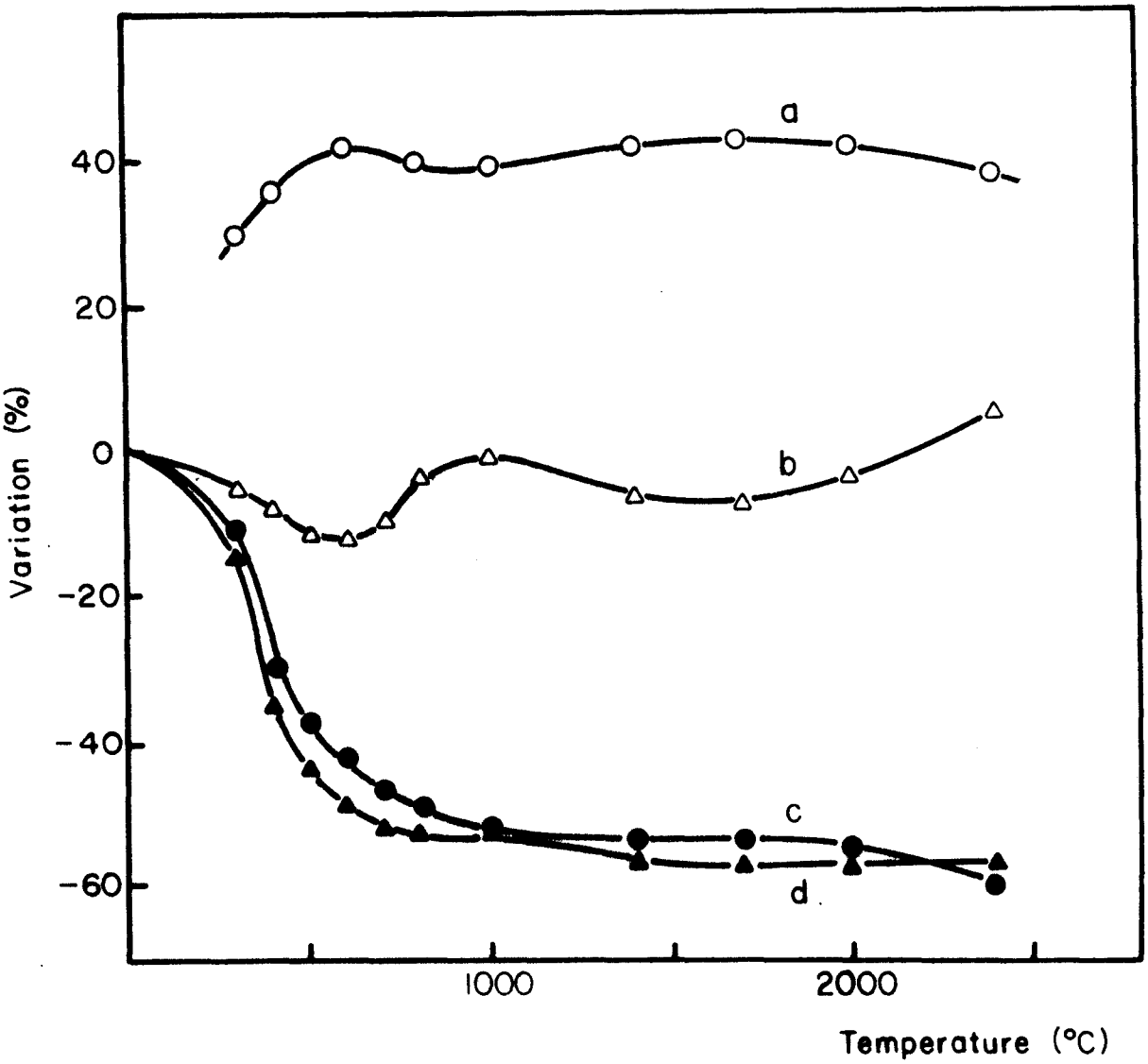

FIGURE 1

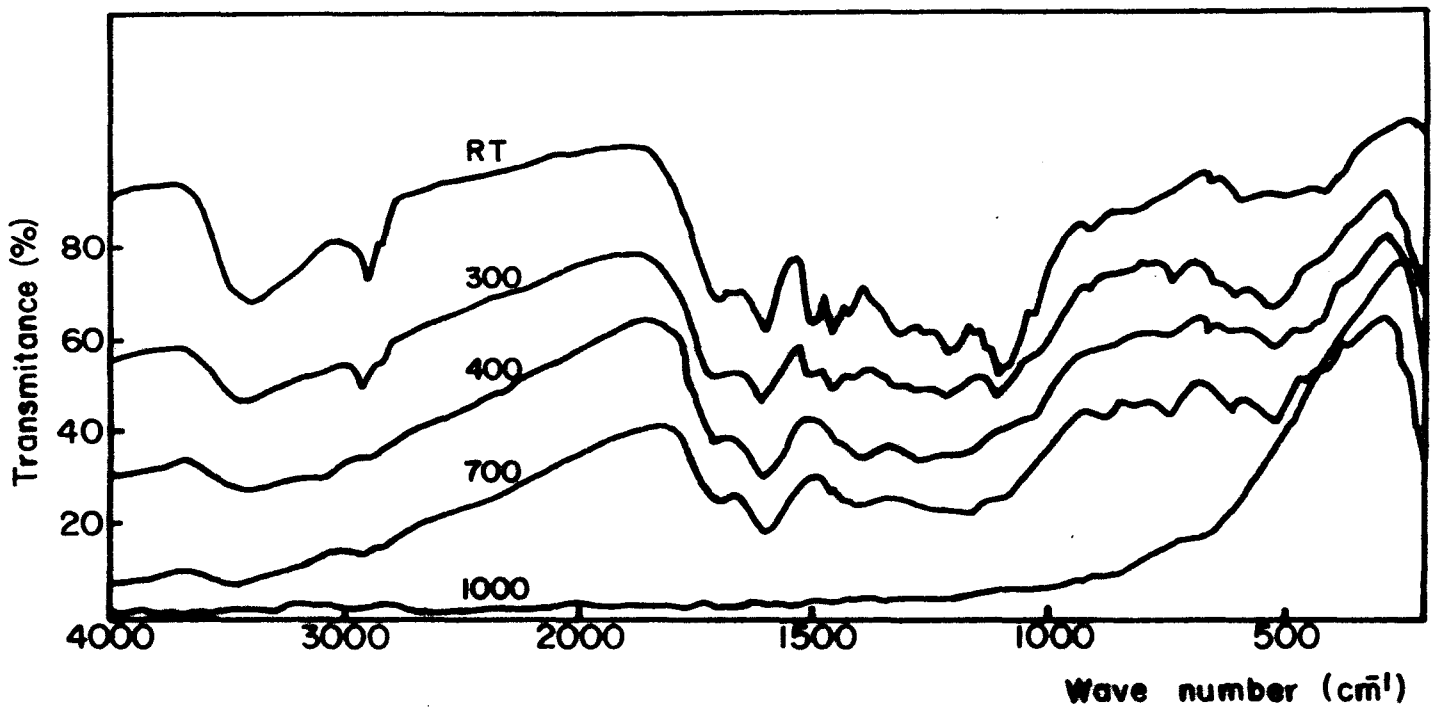
RT
300
400
700
1000
Transmitance (%)
80
60
40
20
4000
3000
2000
1500
1000
500
Wave number (cm⁻¹)

FIGURE 2

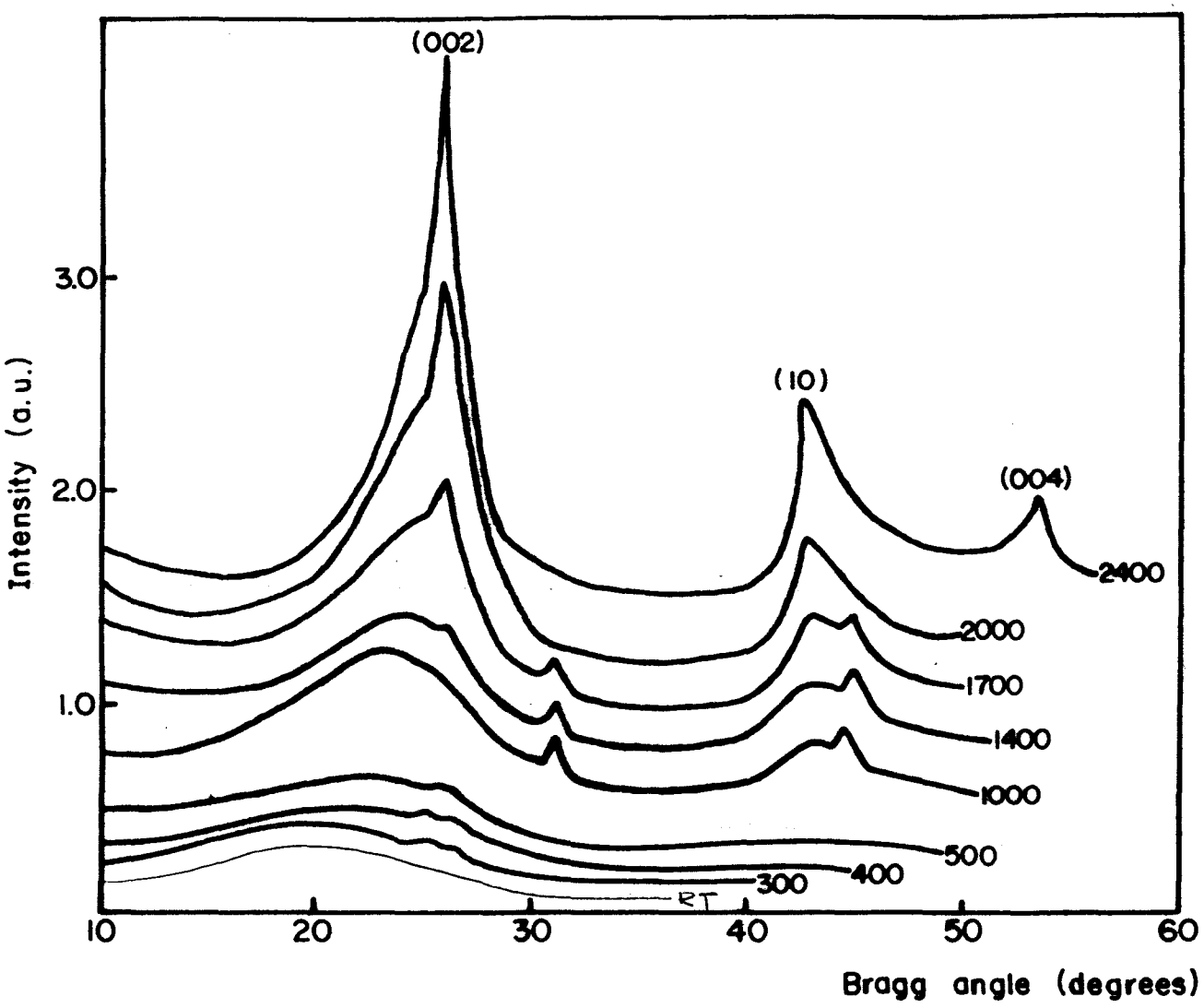
(002)
(10)
(004)
2400
2000
1700
1400
1000
500
400
300
RT
3.0
2.0
1.0
Intensity (a.u.)
10
20
30
40
50
60
Bragg angle (degrees)

FIGURE 3

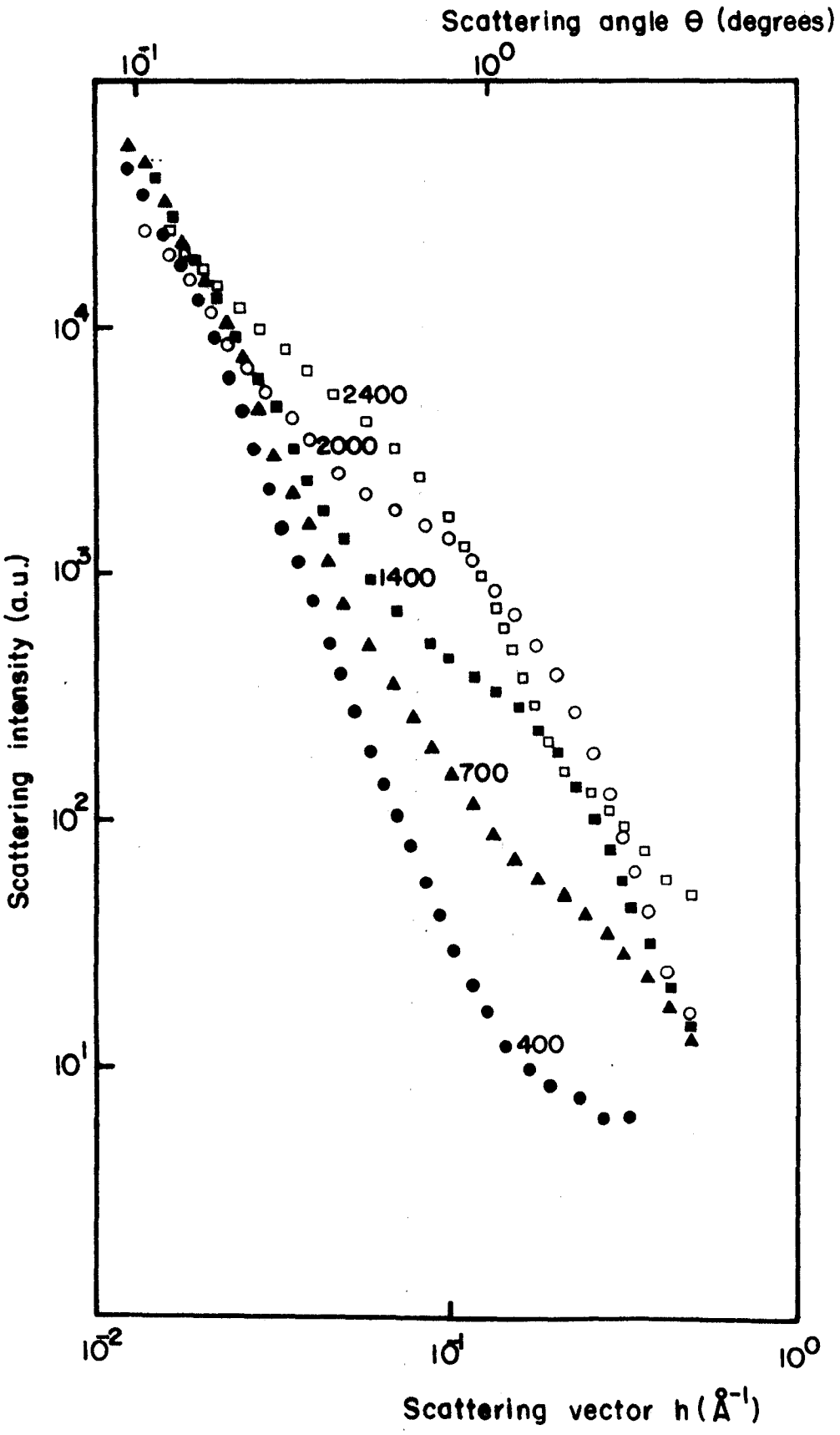
Scattering angle θ (degrees)
10^1
10^0
Scattering intensity (a.u.)
10^4
10^3
10^2
10^1
2400
2000
1400
700
400
10^-2
10^-1
10^0
Scattering vector h (Å^-1)

FIGURE 4

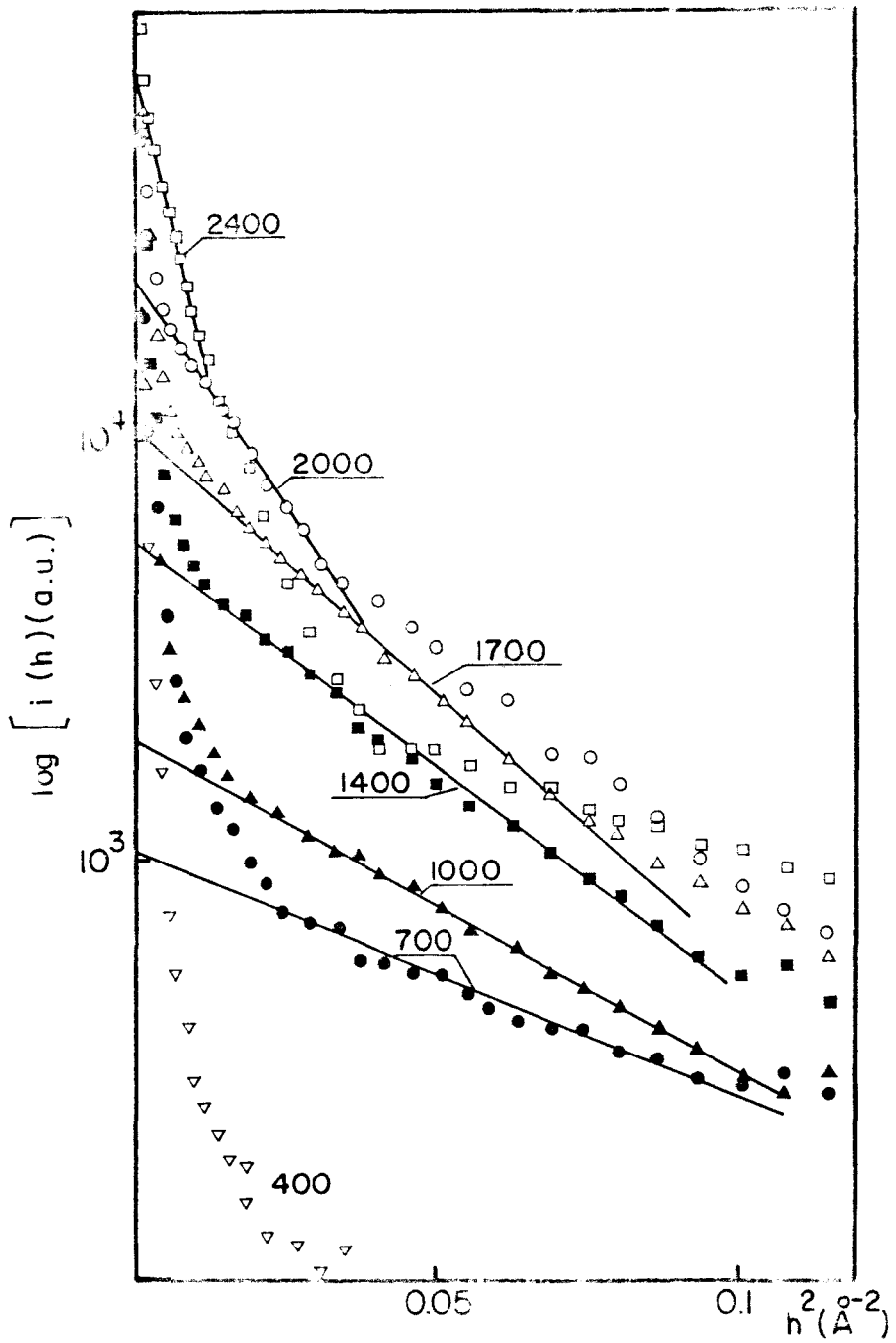

FIGURE 5

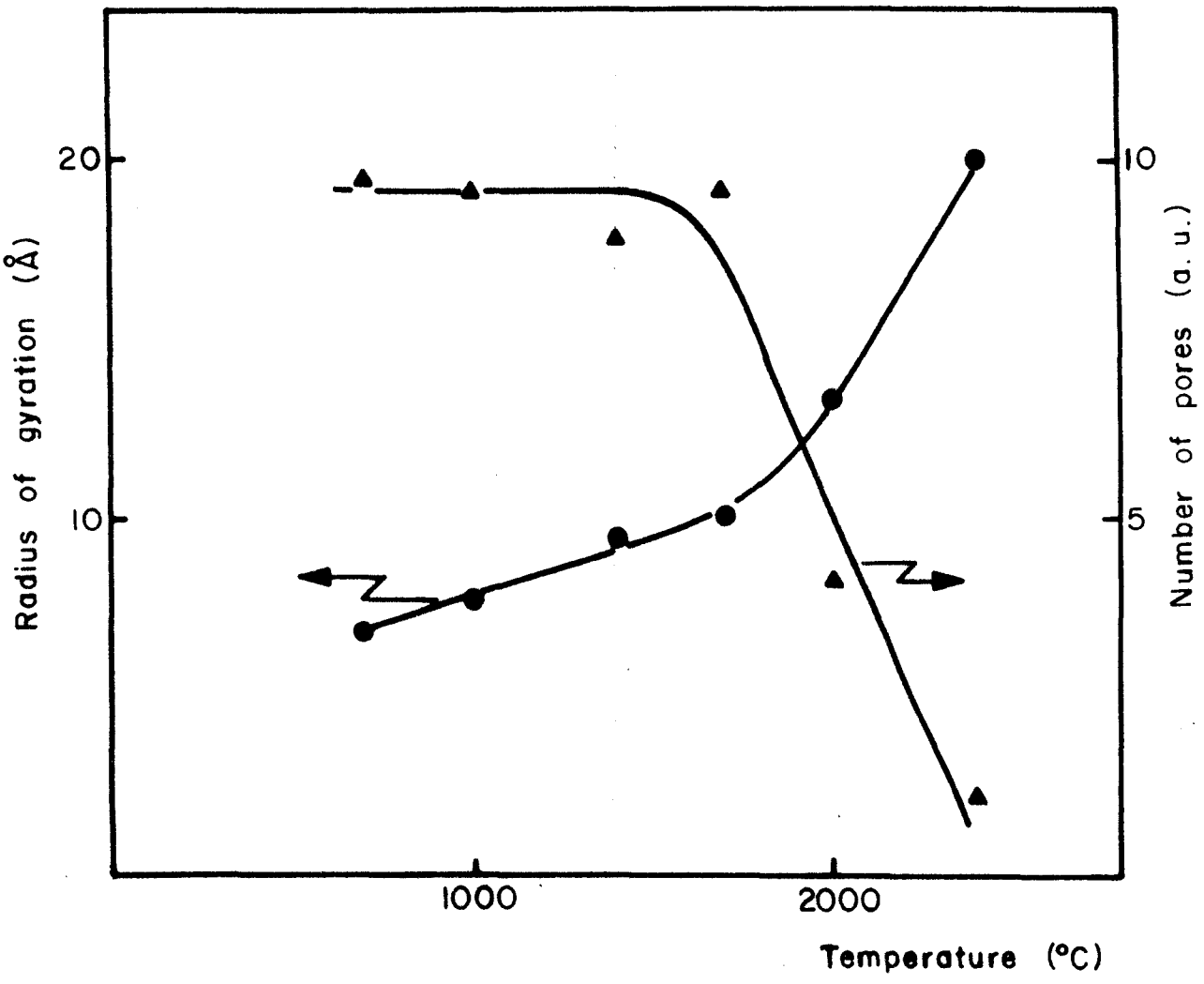
20
10
Radius of gyration (Å)
10
5
Number of pores (a. u.)
1000
2000
Temperature (°C)

FIGURE 6

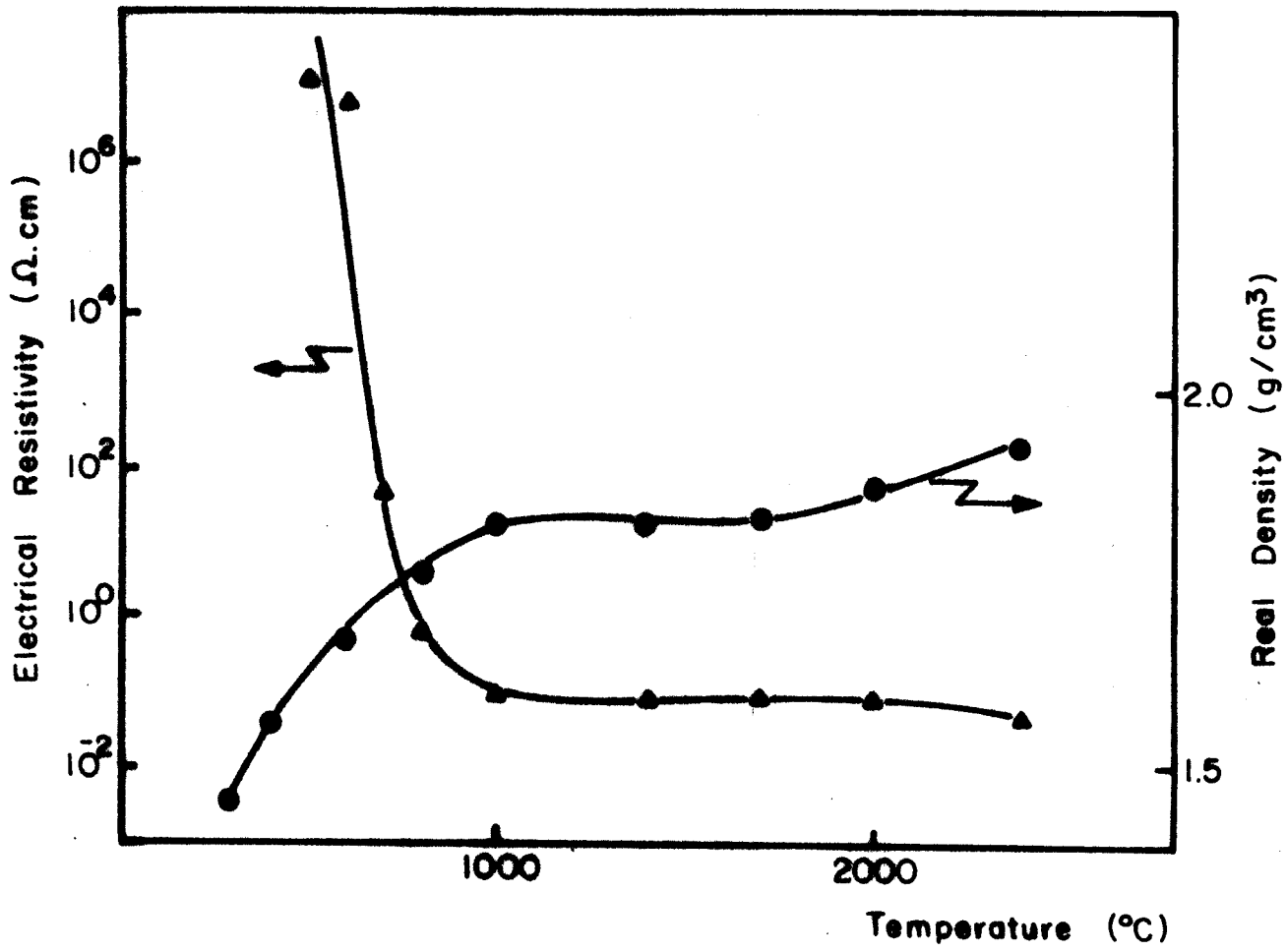
Electrical Resistivity (Ω.cm)
10⁶
10⁴
10²
10⁰
10⁻²
1000
2000
Temperature (°C)
2.0
1.5
Real Density (g/cm³)

FIGURE 7

REFERENCES

1. D.A.I. Gring. *Lignins: Occurence, Formation, Structure and Reactions*. (Edited by K.V. Sarkanen and C.H. Ludwig,- Wiley, Interscience, USA, (1971).

2. C. Otani, H. Polidoro, S. Otani and A. Craievich. To be presented nº 6º CBECIMAT, Rio de Janeiro, Brazil (1984).

3. Sink Float Method - Grafil Test Methods, Test Reference 104.23.

4. H.L. Hergert - *Lignins: Occurrence, Formation, Structure and Reactions*. (Edited by K.V. Sarkanen and C.H. Ludwig), Chap. 4, Wiley, Interscience, USA, (1971).

5. A. Guinier - *Théorie et Technique de la Radiocristallographie*. (Edited by Durot), Paris, (1964).

6. P.W. Schmidt, M. Kalliat and B.E. Cutter. Paper presented at Symposium on Gasification of Chars from Carbonaceous Materials, St. Louis, Missouri, USA, (1984).

7. C.R. Von Bastian, P.W. Schmidt, P.S. Szopa and E.A. McGinnes Jr - *Wood and Fiber*. 4, 185 (1972).

8. A.F. Craievich and E. Dujouny. J. Mat. Sci. 8, 1165 (1973).

9. I. Tomizuka and D.J. Johnson. Yogyo-Kyokai-Shi. 86, 186 (1978).

10. R. Perret and W. Ruland. J. Appl. Cryst. 1, 308 (1968).

11. A. Guinier and G. Fournet. *Small Angle Scattering of X-Rays*. John Wiley, London (1955).

12. P.W. Schmidt. *Private Communication*. (1983).